

# COUNTERING ANTI-FORENSICS TO WAVELET-BASED COMPRESSION

Meijuan Wang<sup>\*</sup>, Zhenyong Chen<sup>\*</sup>, Wei Fan<sup>\*†</sup>, and Zhang Xiong<sup>\*</sup>

<sup>\*</sup>School of Computer Science and Engineering, Beihang University, Beijing 100191, P. R. China

<sup>†</sup>GIPSA-Lab, Grenoble INP, 11 rue des Mathématiques, F-38402 St-Martin d’Hères Cedex, France

## ABSTRACT

Wavelet-based compression is widely used to reduce image redundancy for efficiently storing and transmitting the data. Thus it is an important part in digital image forensics to trace the wavelet-based image compression history. The wavelet-based compression leaves comb-like quantization artifacts in the DWT (Discrete Wavelet Transform) histogram, which however can be disguised using a proper dithering operation. In this paper, standing on the forensic side, we study the joint histogram of DWT coefficients across different levels, whose pattern is robust across a wide range of natural uncompressed images but can be easily destroyed by the wavelet-based compression or the dithering operation used for anti-forensic purposes. By applying the Hough transform to the joint DWT histogram, we derive a 12-dimensional feature vector and a merged discriminating feature. Experimental results demonstrate the effectiveness of the proposed method for differentiating uncompressed images from (anti-forensic) wavelet-based compressed images.

**Index Terms**— Digital image forensics, anti-forensics, wavelet-based compression, joint DWT histogram

## 1. INTRODUCTION

Digital images, one of the most commonly used multimedia on the Internet and in people’s daily life, have greatly facilitated the dissemination of information. Yet, their authenticity is frequently put in doubt, due to the widespread availability of powerful digital cameras and various easy-to-use image editing softwares. Image forensics has therefore emerged as a passive and blind image authentication technique, to restore some trust to digital images. A forger may be able to create a fake image, whose traces are invisible to human naked eyes. However, the statistical change caused by the image modification may be utilized by the forensic investigator for forgery detection, *e.g.*, exposing image forgery via sensor pattern noise estimation [1], revealing traces of image tampering by detecting inconsistencies in lighting [2], and tracing image history by compression [3], median filtering [4], or re-sampling [5].

In order to efficiently store and transmit digital images, image compression is often adopted so as to reduce the image irrelevance and redundancy. Hence, it is an important aspect in the field of image forensics to trace the compression history of one image, *e.g.*, using the methods proposed in [6]. Popular image compression techniques include, JPEG compression where the quantization is carried out in the discrete cosine transform domain, and JPEG2000 or SPIHT (Set Partitioning in Hierarchical Trees) compression where the quantization is performed in the DWT domain. In the literature, digital

image forensics and anti-forensics to JPEG compression has been well studied recently [7, 8, 9, 10, 11, 12, 13]. However, relatively little effort has been made to wavelet-based compression forensics. Stamm *et al.* [7] are the first to propose an anti-forensic method to conceal footprints in one image left by wavelet-based compression. By filling the comb-like quantization artifacts in the DWT histogram using a dithering operation, their method successfully misleads the wavelet-based compression identifying method in [6].

In this paper, we make contributions on the forensic side to wavelet-based compression. Though the dithering based anti-forensic method [7] successfully removes the quantization artifacts in the DWT histogram, it is worth noticing that the image spatial-domain information is not taken into account while adding the dithering signal to the DWT coefficients. The dithering process is rather *random*, thus some intrinsic natural image statistics may be destroyed. Our work is to some extent inspired by [14], which points out that the magnitudes of DWT coefficients at the same spatial location across different levels are highly correlated especially for the typical localized image structures (*e.g.*, edges). Constructing the joint histogram of DWT coefficients across different levels, we study the statistical change in the image caused by the wavelet-based compression or the anti-forensic dithering process [7]. By applying the Hough transform to the joint DWT histogram, we therefore propose a powerful forensic tool capable of discriminating between uncompressed and (anti-forensic) wavelet-based compressed images.

The remainder of this paper is organized as follows. Sec. 2 gives a brief introduction to wavelet-based image compression forensic and anti-forensic techniques. Sec. 3 proposes our forensic method to wavelet-based compression. Experimental results are shown and discussed in Sec. 4. Finally, we draw the conclusion in Sec. 5.

## 2. RELATED WORK

In this section, we briefly review the basics of wavelet-based image compression algorithms, and summarize image forensic and anti-forensic techniques to wavelet-based compression. Without loss of generality, we consider 8-bit grayscale images in this paper.

During the wavelet-based compression, *e.g.*, JPEG2000, and SPIHT, the 2-dimensional DWT transform is firstly applied to transform a given image from the spatial domain to the frequency domain. In the DWT domain, the image is recursively split into  $N$  levels using lowpass and highpass filters. In the  $n$ -th ( $n = 1, 2, \dots, N - 1$ ) level, a lowpass (denoted as  $L_n$ ), a horizontal (denoted as  $H_n$ ), a vertical (denoted as  $V_n$ ) and a diagonal (denoted as  $D_n$ ) subband are respectively computed. Then the  $L_n$  subband from the  $n$ -th level is filtered again to generate the  $L_{n+1}$ ,  $H_{n+1}$ ,  $V_{n+1}$ , and  $D_{n+1}$  subbands in the  $(n + 1)$ -th level. For JPEG2000, the DWT coefficients of the image are scalar-quantized in each subband. Then the resulting quantized DWT coefficients are coded into a bitstream.

This work was supported in part by National Natural Science Foundation of China (No. 61170178, No. 61103094), and in part by National High Technology Research and Development Program (No. 2013AA01A601).

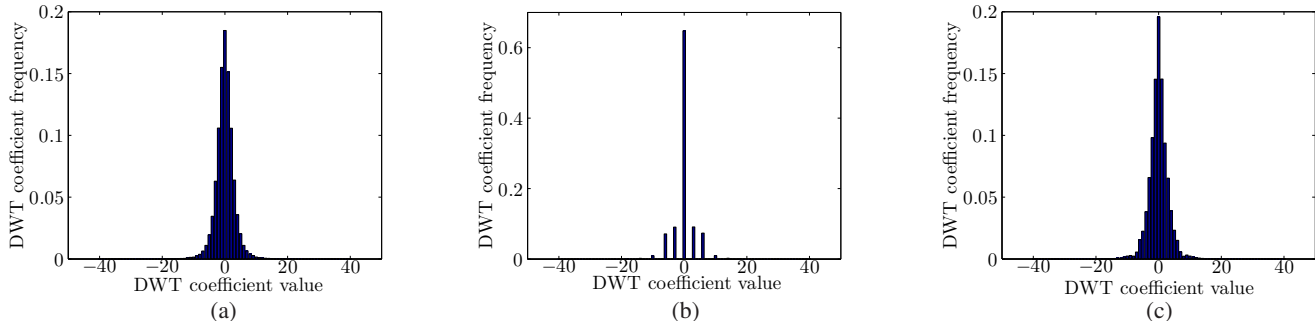


**Fig. 1:** (a) is the  $H_1$  DWT histogram of the classical test image “Lena”. (b) and (c) are the corresponding DWT histograms of (a) after the SPIHT compression at compression rate of 2.5 bpp (bits per pixel), and after the anti-forensic dithering operation [7], respectively.

As to SPIHT [15], the DWT coefficients in each subband are firstly split into bit-planes, for each of which a significance map is generated. A bitstream is therefore constructed by scanning from the most significant map to the least significant one. The lossy compression is achieved by truncating the bitstream to a fixed length. For the decompression process, the DWT coefficients are extracted and reconstructed from the coded bitstream. For JPEG2000, the dequantized DWT coefficient is multiplied by its corresponding quantization step size. Whereas the lost data during the truncation is set to 0 for the bit-plane reconstruction, during the SPIHT decompression. In the end, the 2-dimensional inverse DWT is applied to the DWT coefficients to obtain the decompressed image.

Wavelet-based image compression techniques leave behind similar footprints in the DWT domain. Both of the above described algorithms cluster the DWT coefficients around certain integers. An example can be seen in Fig. 1-(b) comparing with -(a). The quantization artifacts presented in the wavelet-based compressed images can be utilized for forensic purposes to trace the image compression history. Lin *et al.* [6] proposed to model the DWT coefficients using the generalized Gaussian distribution, and the fitting of the DWT histogram is performed using the linear least-squares. The forensic feature is then calculated by computing the correlation between the DWT histogram and its least-square-fit reconstructed one.

In order to remove the wavelet-based compression traces, which can be captured by the forensic feature proposed in [6], Stamm *et al.* [7] proposed to smooth the DWT histogram using a dithering operation. Let  $X$  denote the DWT coefficient in a subband of one wavelet-based compressed image, the DWT coefficient  $Y$  of the anti-forensic forgery is achieved by:

$$Y = X + D, \quad (1)$$

where  $D$  is the dithering signal. The basic assumption of Stamm *et al.*’s dithering based method [7] is that the DWT coefficients of uncompressed images follow the Laplacian distribution in each subband. Therefore,  $D$  is designed in a particular way for  $Y$  to approximate the estimated Laplacian distribution of the uncompressed image. An example dithered DWT histogram is shown in Fig. 1-(c), where no comb-like quantization artifacts appear. The anti-forensic method in [7] can successfully disguise a wavelet-based compressed image as uncompressed under the examination of the forensic method in [6].

Farid and Lyu [16] proposed a forensic method based on the difference between the DWT coefficients and their predictions. A 72-dimensional feature vector is formed, which can be fed to a SVM (Support Vector Machine) to build the detector. This powerful detector can be used in various applications, *e.g.*, steganalysis, and discriminating computer graphics and photograph. We notice that it

can also serve as a forensic detector to differentiate uncompressed images and (anti-forensic) wavelet-based compressed images. In Sec. 4, we will compare our proposed method and Farid and Lyu [16] wavelet-based forensic detectors with experimental results.

### 3. PROPOSED METHOD

The DWT is applied to a given image for transforming it from the spatial domain to the DWT domain. In natural uncompressed images, the substantial power of DWT coefficients tends to be at the same spatial location across different levels [14]. However, this statistical dependence of DWT coefficients may be destroyed by the wavelet-based compression. Moreover, Stamm *et al.*’s anti-forensic dithering operation in Eq. (1) does not particularly take into account the DWT coefficient correlation across different levels. After the dithering signal  $D$  is generated, the adding process to  $X$  is rather *random* without consideration of the DWT coefficient distribution in the spatial domain.

In this section, we study the DWT coefficient dependence across different levels via constructing the joint DWT histogram, whose pattern is very robust for a wide range of natural uncompressed images [14]. We also found this pattern can yet be easily destroyed by the wavelet-based compression or Stamm *et al.*’s anti-forensic dithering operation [7]. We deep study the joint DWT histogram across different levels using the Hough transform. The first four (standardized) moments of the Hough transform parameters are thereafter computed for building the forensic feature vector for wavelet-based forensic purposes.

#### 3.1. Intrinsic Footprints

In order to study the DWT coefficient dependence across different levels. We introduce the “parent” and “child” relationship as in [14]. Consider the  $(r, c)$ -th coefficient  $H_n(r, c)$  in the  $H_n$  subband,  $H_{n+1}(\lceil r/2 \rceil, \lceil c/2 \rceil)$  in the  $H_{n+1}$  subband is defined as its “parent”. In other words,  $H_n(r, c)$  is the “child” of  $H_{n+1}(\lceil r/2 \rceil, \lceil c/2 \rceil)$ . Based on this “parent” and “child” relationship definition, each “child” and its corresponding “parent” are put together as a “parent-child” pair in the horizontal, vertical and diagonal orientations, respectively. Then the joint histogram for the each of the three orientations can be computed. In practice, the “parent” and “child” relationship is more obvious if we transform the DWT coefficients into the log domain. Therefore, in this paper, before the histogram construction, all the DWT coefficient values are processed by taking the logarithm followed by the multiplication by 10. For the sake of brevity, by joint histogram, in this paper we always refer to the log-domain joint histogram.

$$\mathcal{H}^H(x=k, y=l) = \frac{1}{M^H} \sum_{i=1}^{M^H} \delta \left( k - \left[ 10 \times \log_2 |P_i^H| \right], l - \left[ 10 \times \log_2 |C_i^H| \right] \right), \quad k, l \in \mathbb{Z}. \quad (2)$$

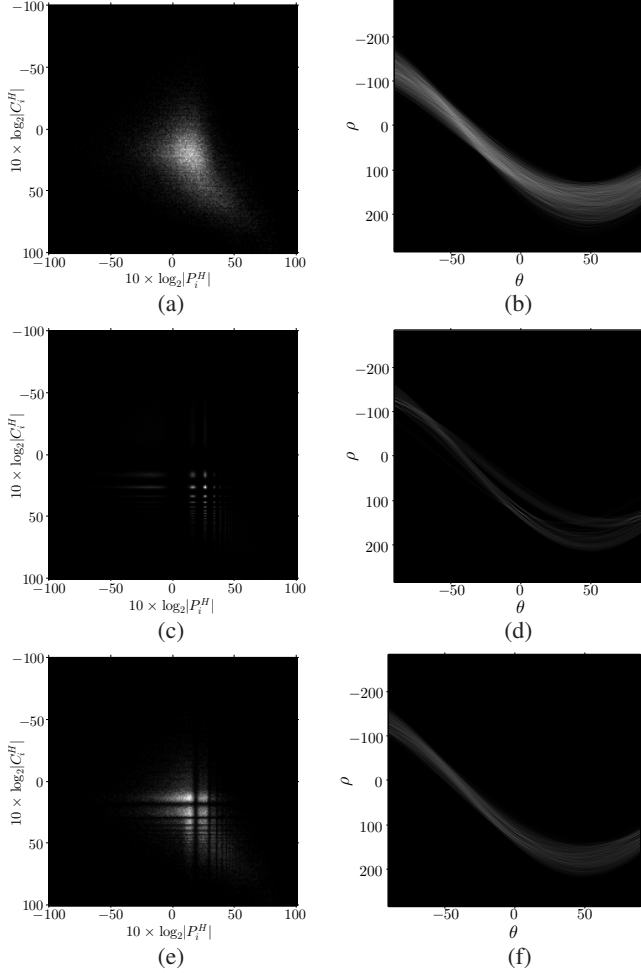


**Fig. 2:** (a) is the truncated, normalized and rounded joint histogram in the horizontal orientation of the “Lena” image. (c) and (e) are the corresponding joint histograms of (a) after the SPIHT compression at the compression rate of 2.5 bpp, and after the anti-forensic dithering operation [7], respectively. (b), (d) and (f) show the Hough transform parameters corresponding to (a), (c) and (e), respectively.

Take the horizontal orientation as an example, the joint histogram  $\mathcal{H}^H$  is computed following Eq. (2). Note that  $\delta$  is the indicator function, and  $\delta(x, y) = 1$  if and only if both  $x = 0$  and  $y = 0$ . Moreover,  $[\cdot]$  is the rounding operation,  $M^H$  is the number of “parent-child” pairs in consideration, and  $P_i^H$  and  $C_i^H$  respectively denote the DWT coefficient values of the “parent” and the “child” in the  $i$ -th “parent-child” pair. Here the superscript “ $H$ ” in  $\mathcal{H}^H$ ,  $M^H$ ,  $P_i^H$  and  $C_i^H$  indicates that they are all for the horizontal orientation. Similarly, the joint histograms  $\mathcal{H}^V$  and  $\mathcal{H}^D$  for the vertical and diagonal orientations can be constructed.

As the substantial frequency of the joint histogram is concentrated in the area where the DWT coefficient magnitude is small, we therefore only consider the central part of the joint histogram with bin values in  $\{-100, -99, \dots, 100\}$ . From an example shown in Fig. 2-(a), we can see that the “parent” and “child” DWT coefficients

are highly correlated in natural uncompressed images. However, this pattern can be destroyed by the wavelet-based compression or the anti-forensic dithering operation [7], as shown in Fig. 2-(c) and -(e). We observe that there is certain linearity in the diagonal direction of the joint histogram. Hence we propose to apply the Hough transform in order to further explore this pattern. Before that, we normalize and round the histogram frequency to integers in the set  $\{0, 1, \dots, 255\}$ . In other words, this pre-processing allows us to treat the joint histogram as a  $201 \times 201$  grayscale image for the Hough transform.

For the line detection in images using the Hough transform, the edge detection is usually applied first. In this paper, the Sobel operator is adopted to perform the edge detection on the truncated, normalized and rounded joint histogram as a pre-processing stage. The Hough transform [17] is used to detect the straight line, which can be represented by a Hough transform parameter pair  $(\rho, \theta)$ . Here  $\rho$  denotes the algebraic distance between the straight line and the origin (defined as the upper-left point  $(-100, -100)$  in the truncated joint histogram), and  $\theta$  is the angle of the vector from the origin to its closest point on the straight line. Therefore, it is possible to associate a Hough transform parameter pair  $(\rho_0, \theta_0)$  with a particular line. The lines going through an arbitrary point in the joint histogram correspond to a curve in the parameter space of the Hough transform. And the number of curves going through the point  $(\rho_0, \theta_0)$  in the Hough transform parameter space determines the number of points on the corresponding line in the joint histogram.

As shown in Fig. 2-(a), -(c) and -(e), we can see that the certain linearity along the diagonal direction is weakened by the wavelet-based compression or the anti-forensic dithering operation [7]. Hence, there are more straight lines and more points on each detected straight line in the joint histogram of uncompressed images than those of wavelet-based compressed images or forgeries created using Stamm *et al.*’s dithering based anti-forensic method [7]. This leads to that the Hough transform parameter space of uncompressed images has more curves and more intersections of curves than those of wavelet-compressed images or Stamm *et al.*’s anti-forensic forgeries [7]. Example results can be seen in Fig. 2-(b), -(d) and -(f). Similar results can also be achieved in the vertical and diagonal orientations. In Sec. 3.2 below, the above described pattern of the Hough transform parameter space will be used to classify uncompressed images and wavelet-based compressed images or Stamm *et al.*’s anti-forensic forgeries [7].

### 3.2. Detecting (anti-forensic) wavelet-based compressed images

Given an image, in order to quantitatively evaluate the Hough transform parameters obtained from the truncated, normalized and rounded joint DWT histogram, we compute its first four (standardized) moments. Then a feature vector  $\mathbf{f}^H$  for the horizontal direction is formed by:

$$\mathbf{f}^H = (\mu^H, \sigma^H, \omega^H, \kappa^H), \quad (3)$$

where  $\mu^H$ ,  $\sigma^H$ ,  $\omega^H$  and  $\kappa^H$  stand for the mean, variance, skewness and kurtosis, respectively. The feature vectors  $\mathbf{f}^V$  and  $\mathbf{f}^D$  for the vertical and diagonal orientations can also be computed similarly. At last, a 12-dimensional feature vector  $\mathbf{f} = (\mathbf{f}^H, \mathbf{f}^V, \mathbf{f}^D)$  is obtained and fed to a SVM to build the forensic detector.

In order to train a SVM-based detector, a set of training data

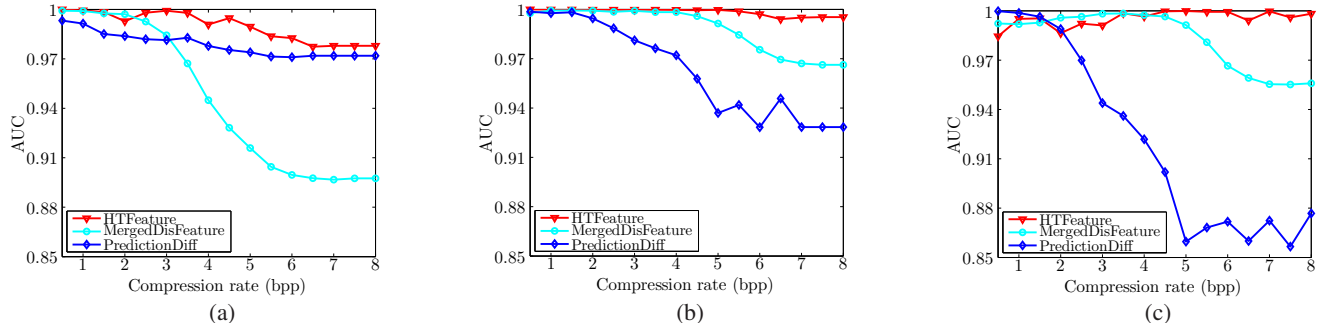


**Fig. 3:** AUC achieved by different forensic detectors for wavelet-based compressed images at different compression rates with or without the application of Stamm *et al.*'s [7] anti-forensic dithering operation. (a) is for JPEG2000 compressed images; (b) is for SPIHT compressed images; and (c) is for anti-forensic SPIHT compressed images [7]. Here, in the legend, “HTFeature” is for the proposed SVM-based detector; “MergedDisFeature” is for the proposed scalar-based detector; while “PredictionDiff” is for the SVM-based detector proposed in [16].

with both positive samples (*i.e.*, (anti-forensic) wavelet-based compressed images) and negative samples (*i.e.*, uncompressed images) is required. In some cases, this condition is not always satisfied. Hence, we further propose a merged discriminating feature (scalar) which can serve as a detector by simple thresholding. The scalar is defined as follows:

$$K = \left| \frac{\mu^H \times \sigma^H}{\omega^H \times \kappa^H} \right| + \left| \frac{\mu^V \times \sigma^V}{\omega^V \times \kappa^V} \right| + \left| \frac{\mu^D \times \sigma^D}{\omega^D \times \kappa^D} \right|, \quad (4)$$

where  $\mu^V$ ,  $\sigma^V$ ,  $\omega^V$ ,  $\kappa^V$ ,  $\mu^D$ ,  $\sigma^D$ ,  $\omega^D$  and  $\kappa^D$  are the first four (standardized) moments of the Hough transform parameters in the vertical and diagonal orientations, respectively. The specific definition of the scalar in Eq. (4) is based on the experimental observation that the skewness and kurtosis values increase, whereas the mean and variance values decrease, when the compression rate decreases. A given image is classified as uncompressed if  $K > \tau$ , where  $\tau$  is a pre-defined threshold.

#### 4. EXPERIMENTAL RESULTS

Our large-scale test is conducted on the UCID-v2 [18] corpus which contains 1338 natural uncompressed images with size  $512 \times 384$ . Without loss of generality, we only consider the luminance component of the image. For generating the wavelet-based compressed images, JPEG2000 and SPIHT algorithms are used and the compression rate varies from 0.5 bpp to 8 bpp with step 0.5. Stamm *et al.*'s anti-forensic forgeries are created from wavelet-based compressed images using the SPIHT compression algorithm, following the experiments in [7]. Therefore, for each compression rate there are three forensic scenarios: differentiating uncompressed images and JPEG2000 compressed images, SPIHT compressed images, or Stamm *et al.*'s anti-forensic SPIHT compressed images [7].

For training the SVM-based detectors using LIBSVM [19] with the Gaussian kernel, we randomly select 669 images from the UCID-v2 corpus for training, whereas the rest of the images are used for testing. The parameters of the SVM are searched using a five-fold cross validation with a multiplication grid as suggested in [20]. As to the proposed scalar in Eq. (4), a detector is built by thresholding.

For each forensic scenario at each compression rate, a ROC (Receiver Operating Characteristic) curve can be achieved for each of the three above described forensic detectors. In this paper, we adopt the AUC (Area Under Curve) as the criterion to evaluate the forensic performance of a detector. From Fig. 3, which compares the proposed method with the wavelet-based forensic method in [16], it can

be seen that the proposed SVM-based detector achieves excellent performance classifying uncompressed images and (anti-forensic) wavelet-based compressed images. As expected, the proposed scalar-based forensic detector does not perform as well as the proposed SVM-based detector. However, it still achieves comparable performance to Farid and Lyu's detector [16], especially when the compression rate is relatively low. The proposed SVM-based detector successfully captures the statistical change in images caused by the wavelet-based compression or Stamm *et al.*'s anti-forensic dithering operation [7], even when the compression rate reaches as high as 8 bpp. The AUC achieved by the proposed SVM-based detector is all greater than 0.97 for all kinds of forensic scenarios and compression rates in consideration. Farid and Lyu's forensic detector [16] also achieves a very good performance, and slightly outperforms both of the proposed two forensic detectors examining Stamm *et al.*'s forgeries when the compression rate is low. Nevertheless, it is worth noticing that our feature vector is 12-dimensional, whereas Farid and Lyu's feature vector is 72-dimensional. The proposed feature vector will greatly facilitate the training procedure of the SVM-based detector, especially when the size of the training set is relatively large.

#### 5. CONCLUSION

In this paper, a powerful wavelet-based forensic method is proposed based on the analysis of DWT coefficient relations across different levels. This DWT coefficient relation is very robust across a wide range of natural uncompressed images, however it can be easily destroyed by the wavelet-based compression or Stamm *et al.*'s dithering based anti-forensic method [7]. We further propose to apply the Hough transform to the joint DWT histogram, thereafter a 12-dimensional feature vector and a merged discriminating feature are derived. Experimental results show that the proposed method performs excellently for classifying uncompressed images and (anti-forensic) wavelet-based compressed images.

Future research shall be devoted to a deeper study of the joint DWT histogram with a more comprehensive analysis than using the Hough transform, and to the compression rate estimation from (anti-forensic) wavelet-based compressed images with comparisons to the JPEG2000 estimation method [21]. Moreover, the proposed forensic method will also be tested on other image datasets besides UCID-v2 [18], considering other wavelet-based compression algorithms besides JPEG2000 and SPIHT. Furthermore, another interesting point may be to use the proposed method to examine other histogram-based anti-forensic methods, *e.g.*, [22].

## 6. REFERENCES

- [1] J. Fridrich, "Digital image forensics using sensor noise," *IEEE Signal Processing Magazine*, vol. 26, no. 2, pp. 26–37, 2009.
- [2] M. K. Johnson and H. Farid, "Exposing digital forgeries in complex lighting environments," *IEEE Trans. on Inf. Forensics Security*, vol. 2, no. 3, pp. 450–461, 2007.
- [3] X. Pan, X. Zhang, and S. Lyu, "Exposing image forgery with blind noise estimation," *ACM Workshop on Multimedia and Security*, pp. 15–20, 2011.
- [4] X. Kang, M. C. Stamm, A. Peng, and K. J. R. Liu, "Robust median filtering forensics using an autoregressive model," *IEEE Trans. on Inf. Forensics Security*, vol. 8, no. 9, pp. 1456–1468, 2013.
- [5] X. Feng, I. J. Cox, and G. Doërr, "Normalized energy density-based forensic detection of resampled images," *IEEE Trans. on Multimedia*, vol. 14, no. 3, pp. 536–545, 2012.
- [6] W. S. Lin, S. K. Tjoa, H. V. Zhao, and K. J. R. Liu, "Digital image source coder forensics via intrinsic fingerprints," *IEEE Trans. on Inf. Forensics Security*, vol. 4, no. 3, pp. 460–475, 2009.
- [7] M. C. Stamm and K. J. R. Liu, "Anti-forensics of digital image compression," *IEEE Trans. on Inf. Forensics Security*, vol. 6, no. 3, pp. 1050–1065, 2011.
- [8] S. Lai and R. Böhme, "Countering counter-forensics: the case of JPEG compression," in *Proc. Int. Conf. on Information Hiding*, 2011, pp. 285–298.
- [9] G. Valenzise, V. Nobile, M. Tagliasacchi, and S. Tubaro, "Countering JPEG anti-forensics," in *Proc. IEEE Int. Conf. Image Process.*, 2011, pp. 1949–1952.
- [10] G. Valenzise, M. Tagliasacchi, and S. Tubaro, "Revealing the traces of JPEG compression anti-forensics," *IEEE Trans. Inf. Forensics Security*, vol. 8, no. 2, pp. 335–349, 2013.
- [11] W. Fan, K. Wang, F. Cayre, and Z. Xiong, "A variational approach to JPEG anti-forensics," in *Proc. IEEE Int. Conf. Acoust., Speech, and Signal Process.*, 2013, pp. 3058–3062.
- [12] W. Fan, K. Wang, F. Cayre, and Z. Xiong, "JPEG anti-forensics using non-parametric DCT quantization noise estimation and natural image statistics," in *Proc. ACM Int. Workshop on Information Hiding and Multimedia Security*, 2013, pp. 117–122.
- [13] W. Fan, K. Wang, F. Cayre, and Z. Xiong, "JPEG anti-forensics with improved tradeoff between forensic undetectability and image quality," *IEEE Trans. on Inf. Forensics Security*, 2014.
- [14] R. W. Buccigrossi and E. P. Simoncelli, "Image compression via joint statistical characterization in the wavelet domain," *IEEE Trans. on Image Process.*, vol. 8, pp. 1688–1701, 1999.
- [15] A. Said and W. A. Pearlman, "A new, fast, and efficient image codec based on set partitioning in hierarchical trees," *IEEE Trans. on Circuits Syst. Video Technol.*, vol. 6, pp. 243–250, 1996.
- [16] H. Farid and S. Lyu, "Higher-order wavelet statistics and their application to digital forensics," *IEEE Workshop on Statistical Analysis in Computer Vision (in conjunction with CVPR)*, 2003.
- [17] P. V. C. Hough, "Method and means for recognizing complex patterns," 1962, US Patent 3,069,654.
- [18] G. Schaefer and M. Stich, "UCID - An uncompressed colour image database," in *Proc. SPIE: Storage and Retrieval Methods and Applications for Multimedia*, 2004, pp. 472–480.
- [19] C.-C. Chang and C.-J. Lin, "LIBSVM: A library for support vector machines," *ACM Trans. Intelligent Systems and Technol.*, vol. 2, pp. 27:1–27:27, 2011.
- [20] P. Pevny, P. Bas, and J. Fridrich, "Steganalysis by subtractive pixel adjacency matrix," *IEEE Trans. on Inf. Forensics Security*, vol. 5, no. 2, pp. 215–224, 2010.
- [21] G. Qadir, X. Zhao, and A. T. S. Ho, "Estimating JPEG2000 compression for image forensics using Benford's Law," in *Proc. SPIE 7723, Optics, Photonics, and Digital Technologies for Multimedia Applications*, 2010, pp. 77230J–1:77230J–10.
- [22] M. Barni, M. Fontani, and B. Tondi, "A universal technique to hide traces of histogram-based image manipulations," in *ACM Workshop on Multimedia and Security*, 2012, pp. 97–104.